Pergamon

Cement and Concrete Research, Vol. 26, No. 7, pp. 1013-1028, 1996

0008-8846/96 $15.00 + .00

PII S0008-8846(96)00089-0

MICROSTRUCTURAL AND MICROANALYTICAL STUDIES OF SULFATE ATTACK. IV. REACTIONS OF A SLAG CEMENT PASTE WITH SODIUM AND MAGNESIUM SULFATE SOLUTIONS

R.S. Gollop and H.F.W. Taylor
Blue Circle Industries PLC
Technical Centre, 305 London Road
Greenhithe, Kent DA9 9JQ, UK

(Refereed)
(Received December 4, 1995; in final form May 7, 1996)

ABSTRACT

Cubes of a blended cement paste that had been stored for 6 months in solutions of Na_2SO_4 or $MgSO_4$ were examined by scanning electron microscopy using backscattered electron imaging and X-ray microanalysis. The blend contained 31% of Portland cement (PC) and 69% of blastfurnace slag (ggbs). The changes observed were broadly similar to those which we have found with a normal PC but less gypsum was formed. The veins of this phase formed near to the faces and edges of the cube stored in Na_2SO_4, and those of gypsum and of brucite in the paste stored in $MgSO_4$, were microstructurally different from those in the PC paste and were less continuous. Decalcification of the C-S-H was marked with $MgSO_4$ but also significant with Na_2SO_4. Matters discussed include the part played by the sulfide released from the slag, the role of CH in external sulfate attack and the reported tendency for materials made with slag cements to soften and disintegrate as a result of sulfate attack rather than to expand.

Introduction

The literature contains many studies on the resistance to sulfate attack of mortars or concretes made using slag cements, but few that deal with the chemical or microstructural changes that take place. Locher (1) reported on the resistance to attack by Na_2SO_4 solution of a wide range of blends made from Portland cement (PC) clinkers, ground granulated blastfurnace slags (ggbs) and gypsum, and made parallel XRD examinations. He found that resistance was improved if more than 65% of the PC was replaced by ggbs, and also at lower degrees of substitution if the ggbs was low in Al_2O_3 (11%), but that it was reduced at low degrees of substitution if the slag was high in Al_2O_3 (18%). For the blends giving high resistance, he concluded from XRD that the amounts of ettringite formed were very small in mortars, but much higher in agitated suspensions. He concluded that formation of ettringite in the sulfate-resistant mortars was largely prevented, either because of low permeability or because the pore structure of the paste was such as to prevent nucleation.

Kobayashi et al. (2) briefly reported XRD and SEM studies on blends of PC and slag that had been stored in $MgSO_4$ solution. Both ettringite and gypsum were detected.

Rasheeduzzafar et al. (3) studied the action of a solution containing sodium and magnesium sulfates on mortars made using PC alone and blended with ggbs or other materials. After 2 years, all showed severe deterioration, which was most marked with the cements containing ggbs (ggbs:PC = 60:40) or microsilica (silica fume). The deterioration was characterised by scaling, spalling and softening rather than expansion and cracking. XRD and SEM showed formation of much gypsum and also of magnesium silicate hydrate (M-S-H), and it was clear that substantial decomposition of C-S-H had taken place. The inferior performance of the cements containing ggbs or microsilica was attributed to the low contents of CH which would otherwise have provided the Ca^{2+} ions needed to form gypsum, thereby protecting the C-S-H from attack. The authors considered that decreased formation of brucite in the case of the cements made using ggbs or microsilica also increased their susceptibility to attack. Other studies have shown that, with plain PC pastes, a quasi continuous, composite layer of brucite and gypsum is formed at the surface (4-6).

Related studies of expansion and strength loss were reported on mortars exposed to Na_2SO_4 solution (3,7,8). In this case, damage took the form primarily of expansion and cracking, and was less marked with the blended cements, including one containing 70% of ggbs. It was concluded that the deterioration was primarily due to ettringite formation and that the lower contents of CH produced by the blended cements in this case improved the resistance, since this phase provided the Ca^{2+} ions needed to form either ettringite or gypsum.

Hemmings et al. (9) reported the results of physical tests and preliminary chemical and microstructural studies on pastes and mortars which had been stored in an Na_2SO_4 solution. Pastes of PC, SRPC (sulfate-resisting Portland cement) and a 50:50 blend of a high C_3A PC with a slag relatively low in Al_2O_3 were studied by XRD, thermal analysis and pore solution analysis. Fracture surfaces and polished sections taken from the mortar prisms of the PC and slag blends were also examined in the SEM. The PC and SRPC pastes were found to contain substantial quantities of gypsum; ettringite could not be detected by XRD or thermal analysis, though SEM showed that a little was present in voids in the PC paste. With the slag blend, in contrast, an ettringite-type phase was clearly present, but no gypsum could be detected. The slag blend showed good resistance to sulfate attack, which was attributed to the low content of CH. This was considered to favour the formation of ettringite in relatively large crystals, which were deposited in the larger pores or voids, where they had little or no expansive effect.

No detailed studies using backscattered electron (BSE) imaging or quantitative X-ray microanalysis of polished sections of pastes or mortars made from slag cements and subjected to external sulfate attack appear to have been reported. In this paper, we describe the results of such an investigation, similar to that reported in Parts 1 and 3 of this series for a normal PC and an SRPC, respectively (6,10). The results relate to a single slag blend, stored in separate solutions of Na_2SO_4 and of $MgSO_4$. The blend was one of those for which Kollek and Lumley (11) reported durability data. In a subsequent paper (12), we consider the effects of variations in the slag composition and proportioning of the blend.

Experimental

A normal Portland cement (BS 12, PC Class 42.5) with Bogue C_3A = 9.6% and equivalent Na_2O = 0.34% was used. Reference 6 gave its full chemical composition and other data. The slag was pelletised; XRD (13) indicated that it contained 89% of glass, with melilite as the only detectable crystalline constituent. Chemical analysis gave SiO_2, 36.8; Al_2O_3, 11.2; Fe_2O_3, 0.4; Mn_2O_3, 0.83; P_2O_5, 0.02; TiO_2, 0.99; CaO, 40.0; MgO, 7.7; SO_3, 0.13; S^{2-}, 0.97; K_2O, 0.47;

Na_2O, 0.35; ignition loss, 0.6; O≡S, -0.5; total, 100.0%; insoluble residue, 0.30%. Though given conventionally as Fe_2O_3 and Mn_2O_3, the Fe and Mn almost certainly occurred in lower oxidation states (Fe^0, Fe^{2+}, Mn^{2+}). Sedigraph techniques gave 47% finer than 15 μm and 19% finer than 5 μm; the specific surface area (Lea and Nurse) was 397 m^2kg^{-1}. The apparent particle density (kerosene displacement) was 2920 kg m^{-3}.

A blend containing 69% of slag was prepared using a dry powder blender, and 25 mm cubes of paste were then made at a water/solids (w/s) ratio of 0.3. These were demoulded after 3 days and stored in deionised water for a further 4 days before being stored in solutions of sodium or magnesium sulfate (0.25 mol l^{-1}) at 20°C. The sulfate solutions were replaced after 3, 6 and 12 months. Immediately prior to each replacement, and also at 24 months, the storage solutions were analysed for Na^+, K^+, Mg^{2+}, Ca^{2+} and SO_4^{2-}, and their pH values determined. At an age of 6 months the material was examined in the scanning electron microscope (SEM) using back-scattered electron (BSE) imaging and X-ray microanalysis. 256 spot analyses of hydrated material were recorded from a cube stored in Na_2SO_4 and 180 from one stored in $MgSO_4$. Cubes were also stored in water for various periods at 20°C and then examined by XRD and thermal analysis. All the techniques of sample preparation and examination were described more fully in Part I (6).

Data for the degree of reaction of the slag in the cubes stored in water were obtained using an EDTA extraction method and are reported elsewhere (14). Typical values were 11% at 1 week, 29% at 4 weeks and 36% at 53 weeks. Expressed as percentages of the glass that have reacted, these values become respectively 12%, 33% and 40%. Interpolation suggests that about 39% of the glass had reacted in 6 months.

The cubes that had been stored in sulfate solutions showed varying degrees of damage at the cube edges. After 6 months' storage, compared with the corresponding PC pastes (6), the degree of damage was similar for cubes stored in Na_2SO_4 and somewhat greater for those stored in $MgSO_4$.

Results

Phase Compositions of Pastes Stored in Water. XRD examination of pastes aged 1, 14, 53 and 105 weeks showed the presence in all cases of C-S-H, hydrotalcite, an Afm phase or phases and minor CH, in addition to residual clinker phases, slag glass and melilite. The principal AFm peak at 1 week had a spacing of 0.88 nm, which approximates to that of monosulfate, and tended to move to lower angles in the older pastes (0.92 nm at 105 weeks). The change is possibly due to increasing S^{2-} substitution as the slag reacts. The term 'hydrotalcite' is used in this paper to denote any phase having a structure based on layers of the type $[Mg_{1-x}Al_x(OH)_2]^{x-}$, with water molecules and a balancing anion in interlayer sites, irrespective of the value of x or the nature of the balancing anion. This phase gave a peak at approximately 0.76 nm which became more intense with age; its assignment was supported by XRD of residues from the EDTA extractions (14), which gave patterns showing additional peaks of a phase of that type. For the paste aged 53 weeks, these had spacings of 0.756 nm (100; 003), 0.382 nm (56; 006), 0.257 nm (49; 012), 0.229 nm (47; 015), 0.194 nm (42; 018) and 0.152 nm (19; 110), where the first number in the parentheses is in each case the relative peak height and the second the Miller indices. Least-squares refinement showed that the hexagonal unit cell had a = 0.3043 nm, c = 2.292 nm. Differential scanning calorimetry of a paste aged 53 weeks, using a heating rate of 10 deg

C min^{-1}, gave endotherms at 150°C (mainly C-S-H), 215°C (AFm), 285°C and 445°C (hydrotalcite) and 575°C (CH). The DSC curve for a paste aged 7 days was similar to the above. Thermogravimetry indicated CH contents of 3-4% at 1-53 weeks, referred to the ignited mass.

Microstructures

Paste stored in Na_2SO_4 solution. The microstructure at the cube edges (Fig. 1A) was similar to that observed with the plain PC after similar treatment (6). A substantial microcrack ran diagonally inwards for some 700 μm from near an edge and there were multiple cracks approximately perpendicular to it. The material in this region was dark in the BSE image, suggesting decalcification. Further in, up to a total depth of some 1.5 mm from the edge, there were further cracks and gypsum veins, individually 10-20 μm wide, which also tended to be perpendicular to the diagonal. The gypsum veins were less prominent than in the PC paste.

At the cube faces in places remote from the edges (Fig. 1B), the microstructure differed from that observed in the paste made from the plain PC. Whereas the latter showed a single vein of gypsum some 100-150 μm below the surface, typically 15-20 μm thick and largely continuous, the slag cement paste showed multiple gypsum veins sub parallel to the surface at depths of 150-250 μm. As with the PC paste, there were cracks both sub parallel to the surface and approximately perpendicular to it. The paste was dark up to a depth of some 50 μm. In places, calcite crystals had formed on the surface.

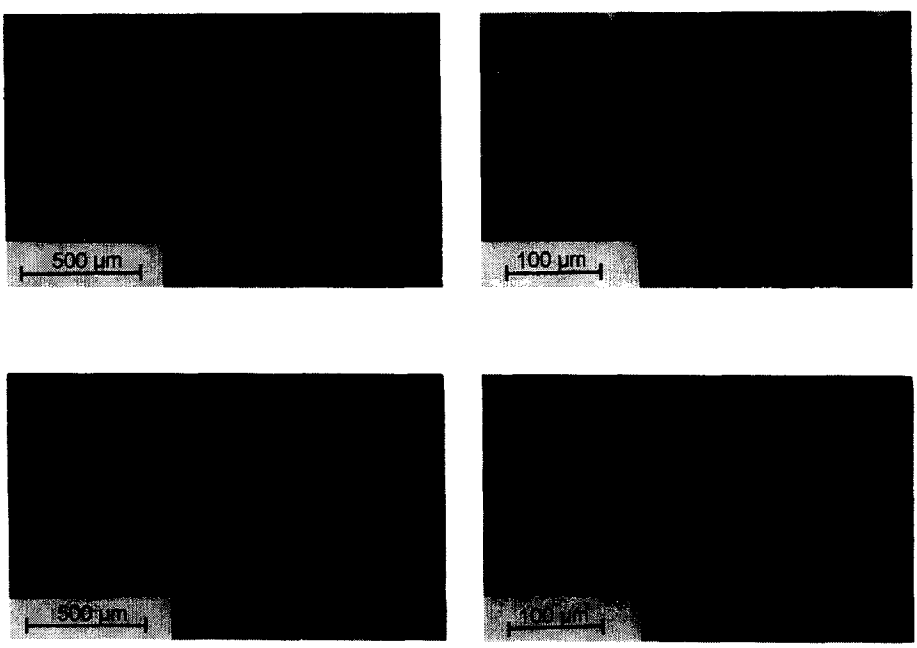

FIG. 1.

Backscattered electron images of polished sections of pastes that had been stored in solutions of Na_2SO_4 or $MgSO_4$. All sections were cut parallel to a cube face; "edge" denotes a field that includes a cube edge and "face" one remote from any such edge.

Paste stored in $MgSO_4$ solution. The microstructure at the cube edges (Fig. 1C) was again broadly similar to that of the PC paste similarly treated (6). The edges bulged outwards, and the material was heavily cracked over distances of up to 500 μm measured along the diagonal. The material near the cube edges was very dark, and was shown by microanalyses to consist largely of M-S-H ($M_3S_2H_2$ approx.; refs. 6 and 10) and residual clinker phases, mainly ferrite. At depths of 300-1000 μm, there were multiple gypsum veins approximately perpendicular to the diagonal.

At the cube faces (Fig. 1D), there was a layer of brucite, typically 10 μm thick, at the surface and one or more discontinuous gypsum veins at depths up to some 100 μm. The material was dark up to a similar depth. This microstructure differs markedly from that observed with the plain PC, which showed a continuous composite surface layer of brucite and gypsum.

X-Ray Microanalyses. Except in the regions within about 200 μm from the face or edge of the cube, in which marked decalcification had occurred, ratios of elements other than Mg, Al, Si and S relative to Ca were generally low and will not be considered. The values rarely exceeded 0.05 for Na/Ca and Fe/Ca, 0.03 for K/Ca, or 0.01 for Ti/Ca and Mn/Ca.

Plots of Si/Ca, S/Ca and Mg/Ca ratios against depth. For cubes stored in each solution, spot analyses were made (i), of the core (> 5 mm from the nearest outer surface), (ii), at various distances inwards from a cube face remote from the edges and (iii), at various distances along a diagonal from a cube edge. Where possible, the distances were recorded with a precision of around ±20 μm, increasing to some ±100 μm at depths above 1 mm. In the heavily cracked region close to the cube edges, the distances could not be defined with any precision. Plots were made of Si/Ca, S/Ca and Mg/Ca ratios against depth. Fig. 2 is that of Si/Ca against depth for spots at points measured inwards from the face or edge of the cube stored in Na_2SO_4 solution. For the core region, the maximum values of around 0.67 represent C-S-H, alone or mixed with hydrotalcite, and lower values represent mixtures in which CH or monosulfate was present in addition or instead. As the surface is approached, the maximum Si/Ca ratios tend to increase from depths of approximately 1 mm, but the Si/Ca ratios do not exceed 1.1 until close below

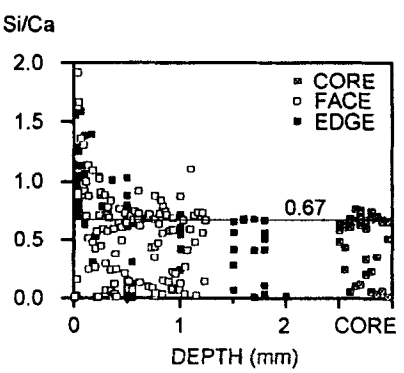

FIG. 2.
Si/Ca atom ratios plotted against depth below a face or edge of the cube stored in Na_2SO_4 solution. Here and in Fig. 3, "core" denotes spots at depths greater than 5 mm from any external surface. These are plotted at arbitrary distances in the direction parallel to the depth axis.

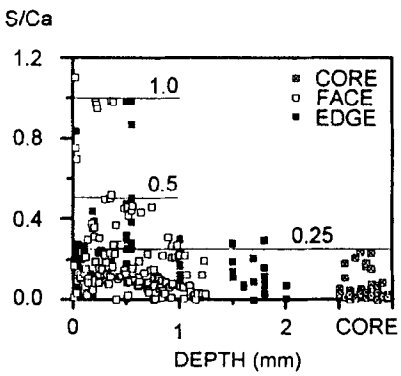

FIG. 3.
S/Ca atom ratios plotted against depth below a face or edge of the cube stored in Na_2SO_4 solution.

the surface. This indicates decalcification, which except in this surface region is a lowering of the Ca/Si ratio of the C-S-H rather than decomposition of that phase. In the outermost 60 μm, much greater increases in the maximum Si/Ca ratio were observed. Some of these values were outside the range shown in Fig. 2, the highest being 17. This indicates a higher degree of decalcification, in which the C-S-H is destroyed and hydrous silica formed.

For the cube stored in $MgSO_4$ solution, the plot of Si/Ca against depth was broadly similar to the above. For the spots at distances measured inwards from the edge of the cube stored in $MgSO_4$, the Si/Ca ratios in the outermost 500 μm were mostly between 10 and 30. These are higher than those generally observed with Na_2SO_4 and were shown to arise from the presence of M-S-H.

Fig. 3 is a plot of S/Ca (sulfur/calcium) against depth for spots at points measured inwards from the face or edge of the cube stored in Na_2SO_4 solution. For the core region, the maximum S/Ca ratios of about 0.25 could be attributed to monosulfate, though, as will be seen, this may be an oversimplification because of the contribution from sulfide originating from the slag. Most of the values, however, are under 0.05, and represent spots consisting essentially of C-S-H, alone or mixed with hydrotalcite. Within about 1 mm from the face, and probably more deeply beneath the edge, there is an upward trend, and a scattering of spots have values between 0.25 and 0.5. These trends show that sulfate is penetrating into the material, and the tendency to a limit at 0.5 suggests that ettringite is being formed. A few spots at depths below 500 μm have S/Ca ratios near to 1.0, and can be attributed to gypsum.

The corresponding plot of S/Ca against depth for the cube stored in $MgSO_4$ solution was broadly similar to that described above. Some spots close to the edge of the cube and consisting almost completely of M-S-H had S/Ca ratios of up to 4. These values could have arisen from the presence of $MgSO_4$ deposited from the storage solution, but because of the low contents of both S and Ca, they are of low precision and possibly not significant.

The plot of Mg/Ca against depth for the cube stored in Na_2SO_4 solution showed no significant variations in the distribution of Mg/Ca ratios apart from a few spots of high Mg/Ca ratio near to the face or edge of the cube, attributable to decalcification. That for the cube stored in $MgSO_4$ solution showed no significant variations other than a few high values attributable

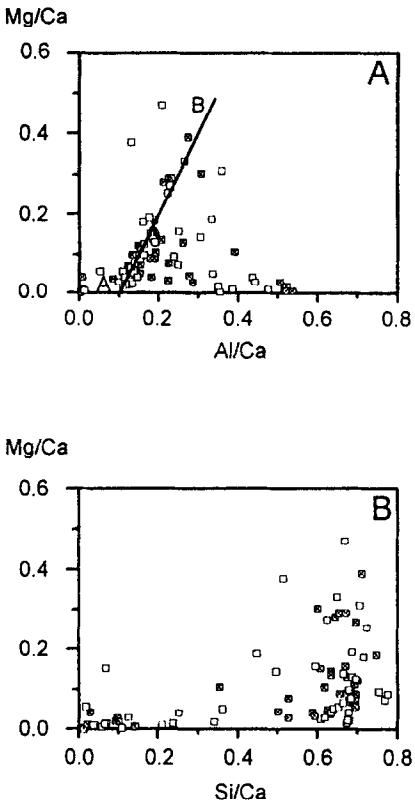

FIG. 4.
Atom ratio plots of Mg/Ca against (A) Al/Ca and (B) Si/Ca for the core regions of the cubes stored in solutions of Na_2SO_4 (open squares) and of $MgSO_4$ (shaded squares).

to brucite in the outermost 70 μm below the cube face, and many due to M-S-H in the outermost 500 μm below the cube edge.

Plots of Mg/Ca against Al/Ca and against Si/Ca. Fig. 4A is a plot of Mg/Ca against Al/Ca for the core region. Spots from the cubes stored in Na_2SO_4 and in $MgSO_4$ are both shown. Following Harrisson et al. (15), the line AB is taken to represent mixtures of C-S-H and hydrotalcite, its slope representing the Mg/Al ratio of that phase and its intercept on the horizontal axis the Al/Ca ratio of the C-S-H. Plots for groups of spots in varying ranges of distance from the face or edge of either cube were similar in form, except for the regions where M-S-H or brucite was present. In all other cases, the plots indicated that the Mg/Al ratio of the hydrotalcite was approximately 2.0 and that the Al/Ca ratio of the C-S-H was approximately 0.1. These results thus suggest that neither the Mg/Al ratio of the hydrotalcite nor the Al/Ca ratio of the C-S-H changes as a result of reaction with sulfate ions.

Fig. 4B is a plot of Mg/Ca against Si/Ca for the core regions of both cubes. Plots for regions of various depths below the face or edge of cubes immersed in either solution were similar.

These results show that the hydrotalcite is very largely present in material having a relatively high Si/Ca ratio. This agrees with observations that the hydrotalcite is closely mixed with C-S-H in the inner product of the slag (15).

The constancy of the Mg/Al ratio of the hydrotalcite makes it possible to use the quantity (Al-Mg/2.0)/Ca as a measure of the ratio of Al to Ca that excludes Al present in hydrotalcite. This approach is derived from that of Wang and Scrivener (16). The observation that the hydrotalcite is largely present in spots of relatively high Si/Ca ratio implies that any errors in the Mg/Al ratio assumed for it will have little effect on the interpretation of analyses for which the Si/Ca ratio is low. These analyses are the most important in determining what other hydrated aluminate phases are present.

Plots of (Al-Mg/2.0)/Ca against Si/Ca and of S/Ca against (Al-Mg/2.0)/Ca. We shall refer to plots of (Al-Mg/2.0)/Ca against Si/Ca as A-type plots and those of S/Ca against (Al-Mg/2.0)/Ca as B-type plots. Fig. 5 shows those for the core regions. Data for the cubes stored in Na_2SO_4 and in $MgSO_4$ are in general agreement. Taken together, the two plots show that most of the spots

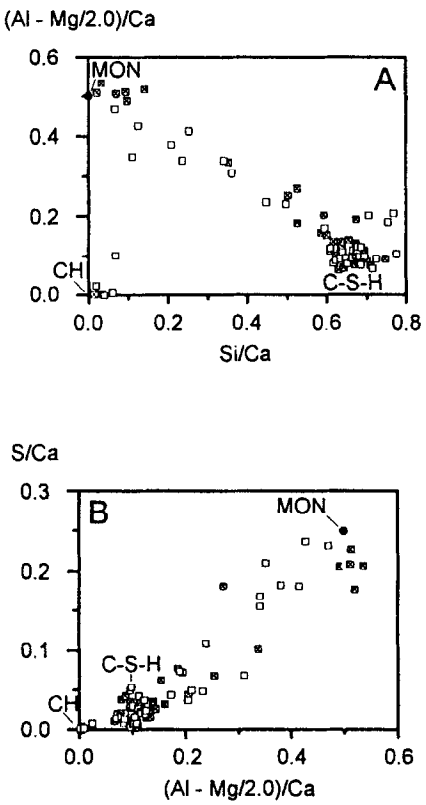

FIG. 5.
"A-type" and "B-type" atom ratio plots for the core regions of the cubes stored in solutions of Na_2SO_4 (open squares) and of $MgSO_4$ (shaded squares). Here and in Fig. 6, MON = AFm phase approximating to monosulfate.

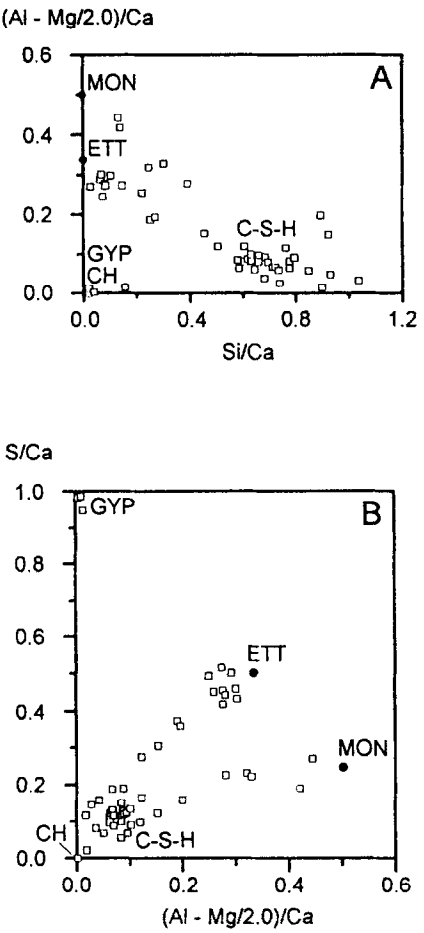

FIG. 6.
"A-type" and "B-type" atom ratio plots for spots at depths of 200-700 μm below a face of the cube stored in Na_2SO_4 solution. GYP = gypsum; ETT = ettringite.

can be assigned either to C-S-H having a Si/Ca ratio ≈ 0.67 (Ca/Si 1.5) and Al/Ca ≈ 0.1, or to an AFm phase with Al/Ca and S/Ca ratios of approximately 0.5 and 0.25, respectively, or to mixtures of the two. A very few spots were of CH. The hydrotalcite which is often present, mostly in the spots with Si/Ca > 0.4, is excluded from these plots by the use of (Al-Mg/2.0)/Ca as one of the variables. For brevity, the AFm phase will be described as monosulfate, though, as was noted earlier, this may be an oversimplification due to the presence of sulfide in the slag.

Similar plots were made for regions of various depth ranges in both cubes. Fig. 6 A and B are examples, and Table 1 gives the principal conclusions derived from all of them. Material having Al/Ca ≈ 0.33 and S/Ca ≈ 0.5 will be described as ettringite, though with reservations similar to those applying to monosulfate. For the cube stored in Na_2SO_4 solution, as the surface or edge of the cube was approached, ettringite replaced monosulfate, CH decreased and ultimately disappeared and the C-S-H was decalcified. These trends continued until the last 150-

TABLE 1
Phases Detected by X-Ray Microanalyses*

Region	Number of analyses	Analyses with Si/Ca > 0.6				Phases detected*	
		Number	Median	% with Si/Ca greater than 0.8	1.2	Major	Minor or trace
Cube stored in Na_2SO_4 solution							
Core	40	24	0.67	0	0	C-S-H, Mon	CH
Face 700-1250 μm	50	21	0.73	29	0	C-S-H, Mon	CH, Ett(?)
Face 200-700 μm	54	27	0.71	22	0	C-S-H, Ett, Mon	Gyp, CH
Face < 200 μm	27	20	1.23	95	55	Decalc	C-S-H(?), Ett(?)
Edge 1000–2000 μm	26	8	0.68	0	0	C-S-H, Mon	CH, Ett
Edge 200–700 μm	25	13	0.80	39	0	C-S-H, Ett	Gyp, Mon, CH
Edge < 200 μm	34	32	1.21	81	50	Decalc	Ett(?), C-S-H(?)
Cube stored in $MgSO_4$ solution							
Core	44	26	0.65	0	0	C-S-H, Mon	CH
Face 700–1000 μm	16	11	0.66	18	0	C-S-H, Mon	CH
Face 200–700 μm	27	15	0.67	7	0	C-S-H, Ett	CH, Mon(?)
Face < 150 μm	8	2	2	100	100	Bru, Gyp,	$CaCO_3$,Decalc
Edge 1100–1500 μm	26	11	0.73	9	0	C-S-H, Mon	CH
Edge 500–1100 μm	36	21	0.70	38	0	C-S-H, Ett, Mon	Gyp
Edge < 500 μm	23	12	17	92	92	M–S–H	Gyp

* Phases other than hydrotalcite. Mon = AFm phase approximating to monosulfate; Ett = ettringite; Gyp = gypsum; M–S–H = magnesium silicate hydrate ($M_3S_2H_2$ approx.); Bru = brucite; Decalc = strongly decalcified material high in SiO_2 and Al_2O_3 (Si/Ca > 1.2).

200 μm below the face or edge. Closer to the surface, spots with high values of Si/Ca and sometimes also of (Al-Mg/2.0)/Ca were abundant. The strongly decalcified and leached productin these regions appeared to consist largely of hydrous silica and alumina with some C-S-H of high Si/Ca ratio (≈1.0) and ettringite. For the cube stored in $MgSO_4$ solution, the results were similar to the above until the last 150 μm below the face, or the last 500 μm below the edge. The products formed in the outermost 150 μm below the face were largely brucite and gypsum, and in the region within 500 μm of the cube edge they were mainly M-S-H and gypsum.

As noted earlier, gypsum was sometimes also encountered at greater depths, both in the cube stored in Na_2SO_4 and in that stored in $MgSO_4$ solution; three analyses of it are shown in Figs 6A and 6B. The gypsum occurred in veins; there was no evidence of its presence in close admixtures with C-S-H or ettringite or both, such as was found in the case of a plain PC (6). In some areas of the cube faces, surface deposits of $CaCO_3$ were present.

Figs 5 and 6 illustrate two further features of the A- and B-type plots. First, in the B-type plots, the apparent S/Ca ratio of the C-S-H tended to increase from values around 0.02 in the core to 0.05-0.10 nearer to the face or edge of the cube. This might be attributable to increasing incorporation of SO_4^{2-} by the C-S-H or hydrotalcite. Second, distinction between mixtures containing monosulfate and those containing ettringite tended to be sharper in the B-type plots than in the A-type plots. This could be explained by the spread of Si/Ca ratios in the partly decalcified C-S-H, which affects only the A-type plots.

Concentrations of Ions in the Storage Solutions. For the Na_2SO_4 solution, the pH values were 12.1, 8.7, 9.5 and 8.1 before the replacements at at ages of 3, 6 and 12 months and at 24 months, respectively. For the $MgSO_4$ solution, the corresponding values were 8.9, 7.7, 7.9 and 7.8. The concentrations of other ions did not differ greatly from those observed with the plain PC (6).

Discussion

Sulfur in Slag Cement Pastes

Sulfide in the hydration products. Granulated or pelletised blastfurnace slags typically contain approximately 1% of sulfur, which is present almost entirely as sulfide. Vernet (17) showed that this is almost entirely contained in the glass and considered that it is released at the rate at which the latter reacts. Several AFm phases containing sulfide have been synthesised (17,18) and when the slag reacts in a blend with PC it probably enters phases of this type (17). An AFm phase containing iron and sulfide has been prepared and is intensely green in colour; its presence probably accounts for the characteristic colour of pastes formed from slag cements (17). Ettringite appears to take only a small proportion of sulfide into solid solution (17). The pore solutions of slag cement pastes contain sulfide and thiosulfate in low concentrations as well as sulfate, but the amounts of sulfide and thiosulfate present could account for only a small proportion of the sulfide released from the slag (17,19,20). Vernet (17) found that sulfide in AFm phases or ettringite is very easily oxidised, but considered it unlikely that any substantial proportion was oxidised in the bulk of a properly made slag cement paste or concrete. Sangha et al. (21) concluded that substantial aerial oxidation took place, but their interpretation of the experimental data was strongly criticised (22). Brückner et al. (23) showed that for a Portland cement made by the Müller-Kühne process and containing 0.65% of S^{2-}, some of that ion was oxidised during hydration to SO_4^{2-} by the Fe^{3+} and Mn^{3+} present in the cement. A similar reaction may well occur with slag cements.

The proportion of the sulfur released into the hydration products of a slag blend in the form of sulfide can be approximately estimated. The slag used in the present investigation contained 0.97% of sulfide; taking into account the proportion of slag in the blend and assuming 39% of the glass to have reacted, this gives 8.4 mmol of S^{2-} released per 100 g of blend. The PC contained 2.3% of SO_3; assuming all this to have reacted, and adding in a small contribution from the slag, this gives 9.3 mmol of SO_4^{2-} per 100 g of blend. Approximately equal amounts of sulfur are thus released as sulfate and sulfide.

Implications for the interpretation of microanalyses. X-ray microanalyses do not distinguish between sulfur in different oxidation states, unless the amounts present are sufficient to allow this to be inferred from analysis totals. This was not possible in the present case. For the core regions of the 6-month old pastes, which had not been attacked by the sulfate solutions, the X-ray microanalyses were approximately consistent with the presence of monosulfate, but some of the sulfur could have been present as sulfide. As noted earlier, the slight increase with age in the principal spacing of the AFm phase in pastes stored in water might be explained in that way, and we have observed more marked changes with blends containing other slags (12). The phase described as monosulfate in the altered regions in which attack had occurred could similarly contain sulfide, though the ratio of sulfate to sulfide necessarily increases due to the uptake of sulfate from the attacking solution.

The possibility was considered that the results were influenced by oxidation in the surface region of the polished section, some 2 μm thick, to which the microanalyses relate. Even though oxidation may be limited in the body of a paste or concrete, it could possibly be complete in this layer. Oxidation might play an important part in the formation of ettringite if the latter cannot accommodate any substantial proportion of sulfide in place of sulfate. If oxidation also took place in agitated suspensions, but not in mortars, it might explain Locher's (1) conclusion that with blends resistant to sulfate attack substantial proportions of ettringite are formed only in agitated suspensions.

We do not exclude the possibility that some oxidation occurred, but consider it unlikely that it could have been a major effect, as the samples were in contact with Hyprez oil during cutting and polishing, and then ultrasonically cleaned with an organic liquid and dried under vacuum prior to carbon coating. In addition, sulfate was supplied by the external solution, so that the effect of any sulfate formed by oxidation would become progressively less significant as attack proceeded. The mortars examined by Locher were made with a plastic aggregate, and he appears to have ground up the entire specimen for removal of this aggregate and subsequent XRD examination. If this is so, the differing observations on mortars and agitated suspensions could probably be explained by dilution of the alteration products in the mortars by unattacked material. Further studies on the extent to which oxidation occurs under various conditions are nevertheless required. One may also ask whether the Al_2O_3 in a sulfide-containing AFm phase is available for reaction with sulfate, and if so, what happens to the sulfide. These questions, too, remain unanswered.

Sulfate attack in the slag blend compared with that in a plain portland cement paste sodium sulfate solution. The results are broadly similar to those which we have obtained with a plain Portland cement paste under similar conditions (6). In both cases, the reaction proceeded by the inward movement of an interface and led to the formation initially of ettringite and later of gypsum. The Ca^{2+} needed in these reactions is provided partly by CH and partly by decalcification of the C-S-H.

The distribution of the gypsum differed from that found with the plain PC. In the latter case, gypsum was present both mixed with the C-S-H on a micrometre scale and in veins, including ones that were essentially continuous some 100-150 μm beneath the cube faces. With the slag blend, the gypsum was detected only in discontinuous veins, which were present at the cube edges and sporadically beneath the cube faces. No gypsum was detected in close admixture with the C-S-H. The quantity of gypsum was probably less than with the plain PC; with some other slag blends, we have found much less or none at all (12). Decreased formation of gypsum from slag blends can perhaps be attributed to the lower content of CH and lower Ca/Si ratio of the C-S-H. Equilibria in the CaO-Al_2O_3-SO_3-H_2O system, reviewed by Brown (24), indicate that for gypsum to be stable, relatively high concentrations of both Ca^{2+} and SO_4^{2-} are required. These could occur in the presence of CH or C-S-H of high Ca/Si ratio, and thus in a PC paste, but not in that of C-S-H of low Ca/Si ratio.

Magnesium sulfate solution. As with Na_2SO_4, the results are broadly similar to those found with the plain PC. The same reactions take place as with Na_2SO_4, but are accompanied by more damaging ones producing brucite, M-S-H and gypsum. Again as with Na_2SO_4, the distribution of the gypsum differed from that found with the plain PC, and this was also the case with the brucite; the continuous, composite layer of the two phases at the cube faces observed with the plain PC was not present, both phases occurring in discontinuous deposits. Bonen and Cohen

(5) observed a similar difference between pastes of a plain PC and of a blend containing microsilica. Decalcification of the C-S-H was much more extensive than with Na_2SO_4 and led to the complete decomposition of that phase at depths up to some 150 μm below the faces, or 500 μm below the edges of the cube. Gypsum can form readily in the paste stored in $MgSO_4$ solution because Mg^{2+} has decomposed the C-S-H, thus releasing Ca^{2+} into the solution.

Physical effects. Expansion and cracking have often been regarded as the principal damaging effects of sulfate attack, but in practice loss of adhesion and strength appear to be more important (25). Several investigators have reported that mortars made with cements containing high proportions of slag frequently show relatively little expansion on exposure to sulfate solutions in laboratory tests, but fail through softening and disintegration (8,11,26). The following discussion of these effects is based very largely on the conclusions of Rasheeduzzafar et al. (3,7) and Al-Amoudi et al. (8), taken in conjunction with the present results. Expansion and cracking are considered to be due, directly or indirectly, to ettringite formation, and loss of adhesion and strength to the destruction of C-S-H, and this last process is considered to be of greater relative importance in the case of slag blends.

Softening and disintegration have also been attributed to gypsum formation. and the term "gypsum corrosion" has been used (27). They are certainly associated with gypsum formation, but there is not necessarily a causal relationship. The C-S-H is what mainly holds the paste, and with it the concrete, together, and it is likely that destruction of this phase is the prime cause of weakening (28). Crystallisation of gypsum may, nevertheless, have a contributory effect.

Ettringite formation. This requires sources of water and of SO_4^{2-}, Ca^{2+}, OH^-, and $Al(OH)_4^-$ ions. The only significant direct source of the $Al(OH)_4^-$ is AFm phase; unreacted slag and clinker phases may be considered indirect sources. As has been seen, Al_2O_3 present in C-S-H or hydrotalcite is not available, and this is also true of ettringite already formed independently of sulfate attack. The microstructural evidence shows that the Ca^{2+} and OH^- are provided initially by dissolution of CH and that the Si/Ca ratio of the C-S-H begins to increase only when the CH has been depleted, or, perhaps, when what remains is not readily available. This applies also to Ca^{2+} used in the formation of gypsum.

Ettringite formation is therefore favoured and likely to be the dominant effect if $Al(OH)_4^-$ and CH are freely available. This situation exists in the case of attack by Na_2SO_4 solution on pastes of PC high in C_3A or of blends containing relatively small proportions of slags high in Al_2O_3. Failure in such cases may therefore be expected to occur by expansion and cracking. Ettringite formation is minimal with SRPC, becase the hydration products are low in Al_2O_3 and much of this is not available (10), and with blends high in slag, because although there is much Al_2O_3 in the system, not much is available (12,29). Ettringite formation is also minimal in blends containing a lower proportion of slag and supplementary calcium sulfate (1,12,30), due to the persistence of ettringite formed on normal hydration.

Destruction of C-S-H. With a sodium sulfate solution, the only reactions are those producing ettringite or gypsum. Decalcification of C-S-H takes place and causes the quantity of C-S-H to decrease. With magnesium sulfate solutions, the marked lowering of pH associated with the precipitation of brucite and M-S-H greatly intensifies this effect. Destruction of C-S-H is also favoured by low or zero contents of calcium hydroxide, which is the preferred source of Ca^{2+} used in the formation of gypsum and thus tends to protect the C-S-H from attack (8).

Calcium hydroxide contents are low or even zero with blended cements of all kinds, and this may be why slag cements tend to fail by weakening and disintegration. There may be other relevant effects. Pastes of slag blends are less permeable than those of plain Portland cements, and this may restrict the penetration by sulfate ions. Microstructural studies (31-33) support evidence from other sources that they contain much fine porosity, and this could possibly enhance the ability of the microstructure to accommodate a greater increase in solid volume without undergoing damage. On the other hand, the absence of the quasi continuous composite surface layer of brucite plus gypsum, formed by PC or SRPC, may contribute to a lowered resistance of slag blends to attack by $MgSO_4$ solutions (3).

Conclusions

1. When a blend containing 69% of blastfurnace slag was stored in 0.25 mol l^{-1} Na_2SO_4 solution, the principal chemical reaction resulted in partial decalcification of the C-S-H and replacement of an AFm phase, loosely described as monosulfate, by ettringite. The results suggested that neither Al^{3+} substituted in the C-S-H, nor that present in hydrotalcite, is available for reaction with sulfate.
2. Storage in 0.25 mol l^{-1} $MgSO_4$ solution produced the same reaction, but the dominant effects in this case were decomposition of the C-S-H and formation of brucite and gypsum in the surface regions below the cube faces and of magnesium silicate hydrate and gypsum at the cube edges.
3. The SO_4^{2-} ions penetrated to a depth of about 1 mm below the cube faces and probably more deeply at the edges. These results are similar to those observed with a sulfate-resisting PC under similar conditions.
4. The microstructural features of the deposits of gypsum, and of the brucite formed on reaction with $MgSO_4$, differed from those observed with the plain PC. The quantity of gypsum formed in the paste stored in Na_2SO_4 solution was probably less for the slag blend.
5. Damage from sulfate attack is attributed partly to decalcification, which weakens the C-S-H matrix, and partly to ettringite formation, which causes expansion and cracking. The first of these effects may be relatively more important with slag blends than with plain PC. This may account for reported tendencies of blends high in slag to fail through disintegration and softening rather than through expansion and cracking.
6. In typical cases of blends high in slag, at least as much sulfur enters the hydration products in sulfide as in sulfate. This leads to some uncertainties regarding the interpretation of chemical and microstructural observations, including those pertaining to sulfate attack. Further data on such matters as the reactions of sulfide-containing AFm phases to form ettringite and the extent to which oxidation of the sulfide occurs under varying conditions are required.

Acknowledgements

The authors wish to thank Blue Circle Industries PLC for permission to publish this study and for sponsoring RSG for an External Ph.D. course at Imperial College, University of London. The work forms part of the programme of research being carried out by RSG under the Public Institutions and Industrial Research Laboratories Scheme at Imperial College, where HFWT is a Visiting Professor. The authors are indebted to Dr G.K. Moir for his encouragement and

advice. Similar thanks are due to the late Professor P.L. Pratt and to Dr K.L. Scrivener, of the Department of Materials, Imperial College. The authors also thank the following colleagues at the Technical Centre for assistance of various kinds: M.J. Coole, M.W. Duggan, P.V. Huggett and the late A.C. Sass.

References

1. F.W. Locher, Zem.-Kalk-Gips **19**, 395 (1966).
2. W. Kobayashi, S. Okabayashi and N. Kataoka, N., in Review of the 28th General Meeting of the Cement Association of Japan, p. 78 (1974).
3. Rasheeduzzafar, O.S.B. Al-Amoudi, S.N. Abduljanwad and M. Maslehuddin, J. Mater. Civil Engnrg **6**, 201 (1994).
4. J. Nielsen, in Symposium on Effects of Aggressive Fluids on Concrete, p. 114. Highway Res. Record (113), National Research Council, Washington DC (1966).
5. D. Bonen and M.D. Cohen, Cem. Concr. Res. **22**, 169 (1992).
6. R.S. Gollop and H.F.W. Taylor, Cem. Concr. Res. **22**, 1027 (1992).
7. Rasheeduzzafar, F.H. Dakhil, A.S. Al-Gahtani, S.S. Al-Saadoun and M.A. Bader, Am. Concr. Inst. Mater. J. **87**, 114 (1990).
8. O.S.B. Al-Amoudi, M. Maslehuddin and M.M. Saadi, Am. Concr. Inst. Mater. J. **92**, 15 (1995).
9. R.T. Hemmings, B.J. Cornelius, W.J. Mikols and M.D. Luther, in Fifth CANMET/ACI International Conference on Fly Ash, Silica Fume, Slag and Natural Pozzolans in Concrete (Milwaukee, USA, 1995), Supplementary Papers, p. 595. American Concrete Institute, Detroit (1995).
10. R.S. Gollop and H.F.W. Taylor, Cem. Concr. Res. **25**, 1581 (1995).
11. J.J. Kollek and J.S. Lumley, in Proc. 5th Int. Conf. Durability of Building Materials and Components (Ed. J.M. Baker, P.J. Nixon, A.J. Majumdar and H. Davies), p. 409. E & FN Spon, London (1991).
12. R.S. Gollop and H.F.W. Taylor, Cem. Concr. Res. **26**, in press (1996).
13. Anon., British Standard BS 6699, Specification for Ground Granulated Blastfurnace Slag for Use with Portland Cement, Appendix D (1992).
14. J.S. Lumley, R.S. Gollop, G.K. Moir and H.F.W. Taylor, Cem. Concr. Res. **26**, 139 (1996).
15. A.M. Harrisson, N.B. Winter and H.F.W. Taylor, Mater. Res. Soc. Symp. Proc. **85**, 213 (1987).
16. S.D. Wang and K.L. Scrivener, Cem. Concr. Res. **25**, 561 (1995).
17. C. Vernet, Silicates Indust. **47**, 85 (1982).
18. W. Dosch and H. Keller, in 6th International Congress on the Chemistry of Cement (Moscow, 1974), Vol. 3, p. 141 (Russ. with Engl. preprint). Stroyizdat, Moscow (1976).
19. P. Longuet, L. Burglen and A. Zelwer, Rev. Matér. Constr. (676), 35 (1973).
20. F.P. Glasser, K. Luke and M.J. Angus, Cem. Concr. Res. **18**, 165 (1988).
21. C.M. Sangha, B.A. Plunkett, P.J. Walden and M.J. Hussaini, Cem. Concr. Res. **22**, 181 (1992).
22. C.A. White, Cem. Concr. Res. **23**, 241 (1993).
23. A. Brückner, R Lück, W. Wieker, A. Winkler, C. Andreae and H. Mehner, Cem. Concr. Res. **22**, 1161 (1992).
24. P.W. Brown, in Materials Science of Concrete I (Ed. J.P. Skalny), p. 73. American Ceramic Society, Westerville, Ohio (1989).
25. P.K. Mehta, in Materials Science of Concrete III (Ed. J. Skalny), p. 105. American Ceramic Society, Westerville, Ohio (1992).
26. C.D. Lawrence, Cem. Concr. Res. **22**, 1047 (1992).
27. I. Biczók, Concrete Corrosion, Concrete Protection (8th. Ed.), pp. 188-197. Akadémiai Kiadó, Budapest (1972).
28. D. Bonen, J. Am. Ceram. Soc. **75**, 2904 (1992).
29. F. Schröder and H.-G. Smolczyk, in F. Schröder, Proc. 5th Int. Symp. Chemistry of Cement (Tokyo, 1968), Vol. 4, p. 149. Cement Association of Japan, Tokyo (1969).

30. R. Kondo in Chemistry of Cement, Proc. 4th Int. Symp. (Washington, 1960), Vol. 2, p. 881. NBS Monograph 43, US Department of Commerce, Washington (1962).
31. Q.L. Feng, E.E. Lachowski and F.P. Glasser, Mater. Res. Soc. Symp. Proc. **137**, 419 (1989).
32. I.G. Richardson and G.W. Groves J. Mater. Sci. **27**, 6204 (1992).
33. Y. Cao and R.J. Detwiler, Cem. Concr. Res. **25**, 627 (1995).